SUPPLEMENTARY MATERIAL

SUPPLEMENTARY MATERIAL AND METHODS

General methodology. Details on general methodology such as ALT and AST activities, H&E staining, OPN, HMGB1 and collagen-I IHC, western blot, DHE, adenoviral infection, mRNA isolation and qPCR for genotyping are described in previous publications from our laboratory [1, 2, 3]. The source of commercially available Abs used in the western blot analysis can be found in Supplementary Table 1. The mouse embryonic skin fibroblast (MEF) cell line was obtained from HMGBiotech (Milan, Italy). Primary hepatocytes from WT, *Opn*$^{-/-}$ and *Hmgb1*$^{\Delta Hep}$ mice injected with either MO or CCl_4; primary HSCs from WT and *Opn*$^{-/-}$ mice and primary rat HSCs were isolated and co-cultured as previously [3, 4]. Nuclear and cytoplasmic proteins were extracted according to the method of Dignam *et al* [5]. Silencing of *Rage* and *Tlrs2/4/9* was performed using conventional siRNA transfection (*Rage* [sc-106985], *Tlr4* [sc-15001] and *Tlr9* [sc-270187] were from Santa Cruz Biotechnology (Santa Cruz, CA); *Tlr2* [sc160440] was from Life Technologies (Carlsbad, CA). ShRNA lentiviral particles to silence *Rage* and *Gfp*, the latter used as control, were from Santa Cruz Biotechnology.

Human samples. Dr. Theise provided paraffin-embedded archived human liver biopsies from de-identified controls (healthy liver explants) and from post-transplant patients with clinically proven HCV-induced fibrosis scored according to the modified Ishak staging for fibrosis which also parallels the Metavir staging system [6]. Even if nowadays is not the standard of care, it was at the time of sample collection. Biopsies were repeated after several years without treatment to evaluate for progression and a new need to treat. These archived samples were IRB approved and no patient information was disclosed.

Induction of liver injury. 10-wks old male WT, *Opn*$^{-/-}$ and *Opn*^{Hep} Tg littermates, *Hmgb1*$^{\Delta Hep}$ and control littermates were used. We used the CCl_4 and the BDL well-established models of

liver fibrosis. In the CCl_4 model, mice were i.p. injected twice a wk with 0.5 ml/kg b. wt. of CCl_4 or equal volume of mineral oil (MO) for 1 mo and they were sacrificed 48 h after the last CCl_4 injection to avoid an acute-phase response over chronic liver injury. In one experiment, mice were co-treated with non-immune IgG or RAGE neutralizing Ab i.p. injected 1 h before every CCl_4 injection for 1 mo. In the BDL model, *Hmgb1*$^{\Delta Hep}$ and control littermates underwent ligation of the common bile duct to induce cholestasis or sham operation (control) and were sacrificed 2 wks later. A set of WT and *Opn*^{Hep} Tg mice was allowed to age for 1 yr and samples were collected for analysis of spontaneous fibrogenesis.

Pathology. In all experiments, the entire left mouse liver lobe was collected and fixed in 10% neutral-buffered formalin and processed into paraffin sections for H&E or IHC. The scores for centrilobular necrosis were 1 = hepatocyte necrosis affecting only zone 3, 2 = in addition to zone 3 necrosis, occasional bridging necrosis was seen and 3 = pronounced bridging and confluent necrosis. Inflammation was noted to be lymphocytes present in the lobules and were scored as follows: 1 = rare foci, 2 = up to 5 foci and 3 when there were >5 foci. Ballooning degeneration was identified when hepatocytes were enlarged in most cases to more than twice the size of its neighboring cells. In addition, the cytoplasmic membrane became rounded instead of the usual hexagonal shape of normal hepatocytes. Most of the cytoplasm appeared empty except for a few irregular wisps of pink material representing damaged cytoplasmic content. The degree of fibrosis ranged from 0 to 4 and patterned after the Brunt system [7]. Briefly, it was as follows: 1 = perisinusoidal/perivenular fibrosis alone, 2 = perisinusoidal/perivenular fibrosis plus portal fibrosis, 3 = bridging fibrosis and 4 = cirrhosis. In the BDL model, ductular reaction was noted to be proliferation of bile ductules at the margins of the portal tracts and the score was 1 = rare bile ductules present, 2 = irregular buds of bile ductules affecting some portal tracts and 3 = when bile ductules are more prominent and affect the majority of portal areas and/or strings of bile ductular epithelial cells were seen intermingled

with hepatocytes. The assessment of the above scores was uniformly performed under 100x magnification.

Immunohistochemistry. The 2A1 OPN Ab was used on IHC and on immunofluorescence. The collagen-I Ab was from Chemicon International (Billerica, MA) and was used on IHC. The HMGB1 Ab was from Abcam and was used on IHC and on immunofluorescence. Specificity of the OPN and HMGB1 Abs was validated using *Opn*$^{-/-}$ and *Hmgb1*$^{\Delta Hep}$ mice, respectively (not shown). The HNF4α and the desmin Abs were from Santa Cruz Biotechnology. In the IHC, reactions were developed using the Histostain Plus detection system (Life Technologies, Waltham, MA). For the OPN, HMGB1 and collagen-I IHC computer-assisted morphometry assessment, the integrated optical density (IOD) was calculated from 10 random fields per section containing similar size portal tracts and central veins at 100x and using Image-Pro 7.0 Software (Media Cybernetics, Bethesda, MD). The results were averaged and expressed as fold-change of the controls. To quantify the cellular localization of HMGB1, the intensity of the red area corresponding to HMGB1 positive staining in the scanned fields was averaged and considered the total HMGB1 positive staining. Next, the software was set to select all nuclei and the intensity of the stained red area corresponding to HMGB1 nuclear positive staining in the scanned fields was averaged and considered the nuclear HMGB1 staining. The nuclear staining was then subtracted from the total staining to calculate the cytoplasmic HMGB1 staining. The results were averaged and expressed as fold-change of the controls. The HMGB1 expression ratios were calculated by morphometry analysis as above in 20 fields per slide at 200x magnification and are expressed as nuclear-to-total and as cytoplasmic-to-total HMGB1 expression.

Cell treatments. Due to the almost full homology of *Hmgb1* and *Opn* between rat and mice, in the majority of the experiments we used primary rat HSCs due to their greater abundance.

Primary rat (250,000 cells/well) or mouse (10,000 cells/well) HSCs were seeded on 6-well or 12-well plates in DMEM/F12 with 10% FBS. Cells were cultured using DMEM-F12 for 4 to 7 d, which was replaced by serum-free DMEM-F12 prior to either endotoxin-free human rOPN treatment (1433-OP-050/CF, R&D Systems, Minneapolis, MN) or rHMGB1 (1690-HM, R&D Systems). Time-course (5 min-48 h) and dose-response (5-500 nM) experiments along with viability assays were carried out to determine the final concentration of rOPN and of rHMGB1 (both at 50 nM) and the best time-point for collagen-I induction (both at 6 h). *Hmgb1*$^{-/-}$ MEFs were used since *Hmgb1*$^{-/-}$ mice are embryonically lethal and HSCs cannot be isolated from them; yet, they have similar phenotype than HSCs. The following treatments were added to the cells 1 h prior to incubation with rOPN and rHMGB1: 0.5 μM wortmannin (Calbiochem, San Diego, CA), 0.5 μM LY294002 (Cell Signaling, Danvers, MA), 0.5 μM apocynin (Fluka, St. Louis, MO), 0.5 μM diphenyleneiodonium chloride (Sigma, St. Louis, MO) or 100 μM cycloheximide (Sigma). The following neutralizing antibodies were added to the cells for 6 h: 5 μg/ml HMGB1 Ab (Shino-Test, Tokyo, Japan) or 5 μg/ml OPN Ab clone 2C5 (provided by Dr. David T. Denhardt). Co-cultures of hepatocytes and HSCs were established as described in earlier publications [4, 8, 9].

Immunofluorescence. Primary mouse HSCs (1,000 cells/well) were seeded in DMEM/F12 with 10% FBS on 12-well plates containing round cover slips on the bottom of the wells. The medium was replaced by serum-free DMEM/F12 overnight prior to the specific treatments following which the cells were gently rinsed with 1x PBS, fixed with 4% paraformaldehyde and permeabilized with 0.5% Triton X-100. After blocking with 5% FBS, the primary Abs used were HMGB1 (Abcam, Cambridge, MA) and collagen-I (Millipore, Billerica, MA) and then the Alexa-488 conjugated goat anti-mouse IgG and Alexa-568 conjugated goat anti-mouse IgG (Life Technologies). Images were acquired by confocal microscopy using a 630x 1.4NA with immersion oil objective at our Microscopy Shared Resource Facility.

Analysis of serum and liver HMGB1 by ESI-LC-MS. All chemicals and solvents used were of the highest available grade (Sigma). Samples were pre-cleared with 50 µl protein G-Sepharose beads for 1 h at 4°C. HMGB1 present in serum or liver was immunoprecipitated with 5 µg of rabbit anti-HMGB1 for 16 h at 4°C as previously described [10]. For the analysis of HMGB1 PTMs, free thiol groups within HMGB1 were alkylated for 90 min with 10 mM iodoacetamide at 4°C. Cysteine residues in disulfide bonds were then reduced with 30 mM dithiothreitol at 4°C for 1 h followed by alkylation of newly exposed thiol groups with 90 mM NEM at 4°C for 10 min. Samples were subjected to trypsin (Promega, Madison, WI) or GluC (New England Biolabs, Ipswich, MA) digestion according to manufacturer's instructions and de-salted using C18 zip-tips (Millipore). Characterization of whole protein molecular weights, acetylated lysine residues or redox modifications on cysteine residues within HMGB1 were determined as described previously by whole protein ESI or tandem mass spectrometry (MS/MS) [11, 12, 13] using either an AB Sciex QTRAP 5500 or an AB SciexTripleTOF 5600 (Sciex Inc., Framingham, MA). Peptide analysis was determined using an AB Sciex QTRAP 5500 equipped with a NanoSpray II source by in-line liquid chromatography using a U3000 HPLC System (Dionex, CA), connected to a 180 µm by 20 mm nanoAcquity UPLC C_{18} trap column and a 75 µm by 15 cm nanoAcquity UPLC BEH130 C_{18} column (Waters, Milford, MA) via reducing unions. A gradient from 0.05% TFA (v/v) to 50% ACN/0.08% TFA (v/v) in 40 min was applied at a flow rate of 200 nL/min. The ion spray potential was set to 2,200-3,500 V, the nebulizer gas to 19 and the interface heater to 150°C.

Vectors transfection. The following vectors were used in the transfection studies: 1) pGFP, an empty vector to serve as a negative control; 2) *Hmgb1*.WT.GFP, containing NLS1 and NLS2 to overexpress HMGB1 and allow response to stimuli that could drive the protein to the cytoplasm;

and 3) *Hmgb1*.NLS1/2(8K→8A).GFP, containing all 8 lysines in the two NLS mutated to alanines and that cannot be acetylated hence resulting in nuclear HMGB1 localization. These mutants were provided by Dr. Marco E. Bianchi (San Raffaele University, Milan, Italy) [14]. HSCs were transfected with these vectors using Lipofectamine 2000 (Life Technologies) as a carrier for 48 h and then treated with rOPN for 6 h.

NOX oxidase activity. HSCs were subjected to three freeze-thaw cycles in 50 mM phosphate buffer containing 1 mM EGTA, 150 mM sucrose and a cocktail of protease inhibitors at pH 7.4. NOX activity was measured using the indirect lucigenin-derived chemiluminescence method [15]. The reaction was initiated by adding 100 µg of protein to 100 µl of reaction buffer containing 100 µM NADPH and 5 µM lucigenin. Luminescence was recorded every 3 min over a period of 20 min in a luminescence reader.

IP:IB. 100 µg of total protein were incubated with 1 µg of HMGB1 Ab for 1 h at 4°C in a rocking device to enable binding between the protein and the Ab. Then, 20 µl of protein A/G PLUS-Agarose (Santa Cruz Biotechnology) were added and incubated for 3 h at 4°C in a rocking device. Samples were washed three times with RIPA buffer and spun down at 12,000 rpm for 2 min. Samples were resuspended in 20 µl of loading buffer, boiled for 7 min and spun down at 12,000 rpm for 2 min. The supernatant was analyzed for acetylated lysines and HMGB1 loading by western blot.

SUPPLEMENTARY RESULTS

***Hmgb1* ablation in hepatocytes partially prevents BDL-induced liver fibrosis in mice.** *Hmgb1*$^{\Delta Hep}$ and control littermates were subjected to BDL. H&E staining and the pathology scores demonstrated less necrosis, inflammation, hepatocyte ballooning degeneration and fibrosis in BDL *Hmgb1*$^{\Delta Hep}$ compared to control littermates (Supplementary Figure 1A, top and Supplementary Figure 1B). *Hmgb1* deletion in hepatocytes was confirmed by IHC in livers from *Hmgb1*$^{\Delta Hep}$ and control littermates and IHC revealed less collagen-I expression in CCl_4-injected *Hmgb1*$^{\Delta Hep}$ compared to control littermates (Supplementary Figure 1A, middle). *Hmgb1* ablation did not affect OPN expression confirming that OPN is upstream of HMGB1 (Supplementary Figure 1A, bottom).

rHMGB1 signals via RAGE to up-regulate collagen-I expression in HSCs. Last, since HMGB1 binds several receptors, of which RAGE [16] and TLRs2/4/9 [17, 18, 19] have been described to play a role in the setting of liver fibrosis, we evaluated whether the HMGB1 effects on collagen-I were receptor-mediated. To this end, we ablated *Rage* or *Tlrs2/4/9* using siRNA. HSCs were treated with rHMGB1 and collagen-I expression was evaluated. RAGE but not TLRs2/4/9 was critical for the effects of rHMGB1 on collagen-I up-regulation in HSCs since western blot analysis showed up-regulation of collagen-I following rHMGB1 treatment but not after *Rage* ablation (Supplementary Figure 2).

Aging *Opn*^{Hep} Tg mice show elevated HMGB1 expression and develop spontaneous fibrosis. We previously showed that *Opn*^{Hep} Tg mice developed spontaneous liver fibrosis over time in the absence of an exogenous profibrogenic stimuli [1], which was confirmed by western blot analysis for collagen-I protein (Supplementary Figure 3A). Thus, we asked whether overexpression of OPN in hepatocytes could also up-regulate HMGB1 expression and perhaps determine its cellular compartmentalization in these mice. We found significant increase in OPN

and HMGB1 expression as depicted by western blot, IHC and morphometry analysis (Supplementary Figure 3B-3C) along with a decrease in the ratio of nuclear-to-total and an increase in the ratio of cytoplasmic-to-total HMGB1 protein expression (Supplementary Figure 3D) in aging *Opn*^{Hep} Tg compared to WT mice.

SUPPLEMENTARY REFERENCES

1 Urtasun R, Lopategi A, George J, Leung TM, Lu Y, Wang X*, et al.* Osteopontin, an oxidant stress sensitive cytokine, up-regulates collagen-I via integrin alpha(V)beta(3) engagement and PI3K/pAkt/NFkappaB signaling. Hepatology 2012;**55**:594-608.

2 Wang X, Lopategi A, Ge X, Lu Y, Kitamura N, Urtasun R*, et al.* Osteopontin induces ductular reaction contributing to liver fibrosis. Gut 2014;**63**:1805-18.

3 Ge X, Antoine DJ, Lu Y, Arriazu E, Leung TM, Klepper AL*, et al.* High mobility group box-1 (HMGB1) participates in the pathogenesis of alcoholic liver disease (ALD). The Journal of biological chemistry 2014;**289**:22672-91.

4 Nieto N, Friedman SL, Cederbaum AI. Stimulation and proliferation of primary rat hepatic stellate cells by cytochrome P450 2E1-derived reactive oxygen species. Hepatology 2002;**35**:62-73.

5 Dignam JD, Lebovitz RM, Roeder RG. Accurate transcription initiation by RNA polymerase II in a soluble extract from isolated mammalian nuclei. Nucleic acids research 1983;**11**:1475-89.

6 Theise ND. Liver biopsy assessment in chronic viral hepatitis: a personal, practical approach. Modern pathology : an official journal of the United States and Canadian Academy of Pathology, Inc 2007;**20 Suppl 1**:S3-14.

7 Kleiner DE, Brunt EM, Van Natta M, Behling C, Contos MJ, Cummings OW*, et al.* Design and validation of a histological scoring system for nonalcoholic fatty liver disease. Hepatology 2005;**41**:1313-21.

8 Mormone E, Lu Y, Ge X, Fiel MI, Nieto N. Fibromodulin, an oxidative stress-sensitive proteoglycan, regulates the fibrogenic response to liver injury in mice. Gastroenterology 2012;**142**:612-21 e5.

9 Nieto N, Friedman SL, Cederbaum AI. Cytochrome P450 2E1-derived reactive oxygen species mediate paracrine stimulation of collagen I protein synthesis by hepatic stellate cells. The Journal of biological chemistry 2002;**277**:9853-64.

10 Antoine DJ, Williams DP, Kipar A, Jenkins RE, Regan SL, Sathish JG*, et al.* High-mobility group box-1 protein and keratin-18, circulating serum proteins informative of acetaminophen-induced necrosis and apoptosis in vivo. Toxicological sciences : an official journal of the Society of Toxicology 2009;**112**:521-31.

11 Antoine DJ, Jenkins RE, Dear JW, Williams DP, McGill MR, Sharpe MR*, et al.* Molecular forms of HMGB1 and keratin-18 as mechanistic biomarkers for mode of cell death and prognosis during clinical acetaminophen hepatotoxicity. Journal of hepatology 2012;**56**:1070-9.

12 Nystrom S, Antoine DJ, Lundback P, Lock JG, Nita AF, Hogstrand K*, et al.* TLR activation regulates damage-associated molecular pattern isoforms released during pyroptosis. The EMBO journal 2013;**32**:86-99.

13 Yang H, Lundback P, Ottosson L, Erlandsson-Harris H, Venereau E, Bianchi ME*, et al.* Redox modification of cysteine residues regulates the cytokine activity of high mobility group box-1 (HMGB1). Molecular medicine 2012;**18**:250-9.

14 Bonaldi T, Talamo F, Scaffidi P, Ferrera D, Porto A, Bachi A*, et al.* Monocytic cells hyperacetylate chromatin protein HMGB1 to redirect it towards secretion. The EMBO journal 2003;**22**:5551-60.

15 Skatchkov MP, Sperling D, Hink U, Mulsch A, Harrison DG, Sindermann I*, et al.* Validation of lucigenin as a chemiluminescent probe to monitor vascular superoxide as well as basal vascular nitric oxide production. Biochemical and biophysical research communications 1999;**254**:319-24.

16 Goodwin M, Herath C, Jia Z, Leung C, Coughlan MT, Forbes J*, et al.* Advanced glycation end products augment experimental hepatic fibrosis. Journal of gastroenterology and hepatology 2013;**28**:369-76.

17 Miura K, Yang L, van Rooijen N, Brenner DA, Ohnishi H, Seki E. Toll-like receptor 2 and palmitic acid cooperatively contribute to the development of nonalcoholic steatohepatitis through inflammasome activation in mice. Hepatology 2013;**57**:577-89.

18 Vespasiani-Gentilucci U, Carotti S, Perrone G, Mazzarelli C, Galati G, Onetti-Muda A*, et al.* Hepatic toll-like receptor 4 expression is associated with portal inflammation and fibrosis in patients with NAFLD. Liver international : official journal of the International Association for the Study of the Liver 2015;**35**:569-81.

19 Miura K, Kodama Y, Inokuchi S, Schnabl B, Aoyama T, Ohnishi H*, et al.* Toll-like receptor 9 promotes steatohepatitis by induction of interleukin-1beta in mice. Gastroenterology 2010;**139**:323-34 e7.

SUPPLEMENTARY TABLE

Supplementary Table 1. List of commercially available Abs used.

Target	Ab	Source
Acetylated Lysines	9441	Cell Signaling
Actin	sc-1616	Santa Cruz Biotechnology
Akt1/2/3	sc-1618	Santa Cruz Biotechnology
Calnexin	sc-6465	Santa Cruz Biotechnology
Collagen-I	MAB3391	Chemicon
Desmin	sc-23879	Santa Cruz Biotechnology
GAPDH	sc-20357	Santa Cruz Biotechnology
HDAC1	5356	Cell Signaling
HDAC2	5113	Cell Signaling
HDAC3	3949	Cell Signaling
HDAC4	7628	Cell Signaling
HDAC5	2082	Cell Signaling
HDAC6	7558	Cell Signaling
HMGB1 (IHC/ICC, IF)	ab18256	Abcam
HMGB1 (WB)	sc-56698	Santa Cruz Biotechnology
HNF4α	sc-6556	Santa Cruz Biotechnology
Nucleoporin p62	610497	BD Biosciences
OPN	sc-21742	Santa Cruz Biotechnology
p300	ab3164	Abcam
p-Akt1/2/3	sc-7985-R	Santa Cruz Biotechnology
PCAF	3378	Cell Signaling
PI3K	sc-7189	Santa Cruz Biotechnology
RAGE	sc-5563	Santa Cruz Biotechnology
RAGE	AF1179	R&D Systems
β-Tubulin	T4026	Sigma

SUPPLEMENTARY FIGURES

Supplementary Figure 1. *Hmgb1* ablation in hepatocytes partially prevents BDL-induced liver fibrosis in mice. *Hmgb1*$^{\Delta Hep}$ and control littermates were bile duct ligated for 2 wks. H&E staining **(A, top)** and pathology scoring **(B)** show lower necrosis, inflammation, hepatocyte ballooning degeneration, fibrosis and ductular reaction in *Hmgb1*$^{\Delta Hep}$ compared to control littermates. IHC shows reduced HMGB1 and collagen-I deposition in livers from BDL *Hmgb1*$^{\Delta Hep}$ compared to control littermates **(A, middle)** whereas OPN expression remained similar **(A, bottom)**. The results are expressed as fold-change of the MO-injected control littermates, which are assigned a value of 1 and are mean values ± SEM; *n*=8/group. •*p*<0.05, ••*p*<0.01 and •••*p*<0.001 for BDL *Hmgb1*$^{\Delta Hep}$ *vs.* control littermates.

Supplementary Figure 2. rHMGB1 signals via RAGE to up-regulate collagen-I expression in HSCs. *Rage* or *Tlrs2/4/9* were ablated using siRNA. HSCs were treated with rHMGB1 and collagen-I expression was evaluated by western blot. The results are expressed as fold-change of the scrambled siRNA control, which is assigned a value of 1 and are mean values.

Supplementary Figure 3. Aging *Opn*^{Hep} Tg mice show elevated HMGB1 expression and develop spontaneous fibrosis. OPN, HMGB1 and collagen-I expression in livers from aging *Opn*^{Hep} Tg compared to WT mice. Western blot analysis for OPN, HMGB1 and collagen-I in total liver from 1 yr old WT and *Opn*^{Hep} Tg mice. The results are expressed as fold-change of the WT mice, which are assigned a value of 1. Results are mean values ± SEM. n=8/group. •••*p*<0.001 for *Opn*^{Hep} Tg *vs.* WT mice **(A)**. IHC analysis of OPN (yellow arrows) and HMGB1 (green arrows) in liver from 1 yr old WT and *Opn*^{Hep} Tg mice **(B)**. Total OPN and HMGB1 morphometry analysis **(C)** and quantification of total, nuclear and cytoplasmic as well as the ratios of nuclear-to-total and of cytoplasmic-to-total HMGB1 **(D)**. The results from the morphometry analysis are

expressed as fold-change of the WT mice, which are assigned a value of 1 and are shown as mean values ± SEM. n=8/group. ••p<0.01 and •••p<0.001 for *Opn*^{Hep} Tg *vs.* WT mice.

Supplementary Figure 4. Proposed mechanism. We previously demonstrated that chronic liver injury and reactive oxygen species induce OPN expression in hepatocytes, HSCs, biliary epithelial cells and oval cells. We showed that OPN engages $\alpha_v\beta_3$ integrin and signals via the PI3K-pAkt1/2/3-NFκB pathway leading to up-regulation of intra- and extracellular collagen-I protein in HSCs (black and white-labeled pathway, *Hepatology* 2012;55(2):594-608). We also established that OPN reduces hepatocyte proliferation and activates the oval cell compartment giving rise to biliary epithelial cells. Furthermore, we identified that OPN increases and/or maintains TGFβ expression in biliary epithelial cells, which along with OPN, signals to HSCs to increase their pro-fibrogenic potential (black and white-labeled pathway, *Gut* 2014;63(11):1805-18). In the present study, we demonstrate significant co-induction of OPN and HMGB1 following liver injury. Additionally, we show that OPN is upstream of HMGB1 in hepatocytes and HSCs. Our hypothesis was that OPN could participate in the pathogenesis of liver fibrosis by increasing HMGB1 to up-regulate collagen-I expression. We now show that well-established liver fibrosis along with marked induction of HMGB1 occurs in CCl_4-injected *Opn*^{Hep} Tg yet it is less in WT and almost absent in *Opn*$^{-/-}$ mice. *Hmgb1* ablation in hepatocytes (*Hmgb1*$^{\Delta Hep}$) protects from CCl_4-induced liver fibrosis. Co-culture with hepatocytes that secrete OPN plus HMGB1 and challenge with either rOPN or rHMGB1 enhances collagen-I expression in HSCs, which is blunted by neutralizing Abs or by *Opn* and *Hmgb1* ablation. rOPN induces acetylation of HMGB1 in HSCs due to increased NADPH oxidase activity and the associated decrease in HDACs1/2 leading to up-regulation of collagen-I. Last, we demonstrate that rHMGB1 signals via RAGE activating the PI3K-pAkt1/2/3 pathway to up-regulate collagen-I (Please, see the strategies used to prove our hypothesis written in blue font).

A

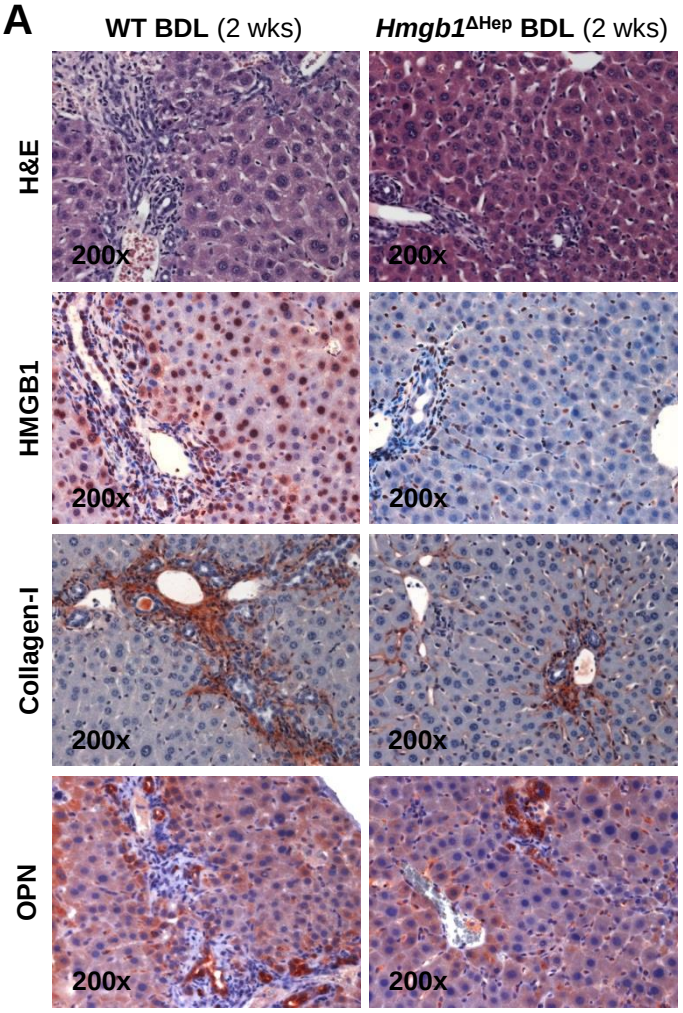

B

	Necrosis	Inflammation	Ballooning	Fibrosis	Ductular reaction
WT + BDL	0.79±0.18	1.86±0.07	0.43±0.02	2.96±0.12	3.42±0.36
***Hmgb1*$^{\Delta Hep}$ + BDL**	0.47±0.11•	1.21±0.14•	0.25±0.06•	1.35±0.15••	1.26±0.14•••

Supplementary Figure 1

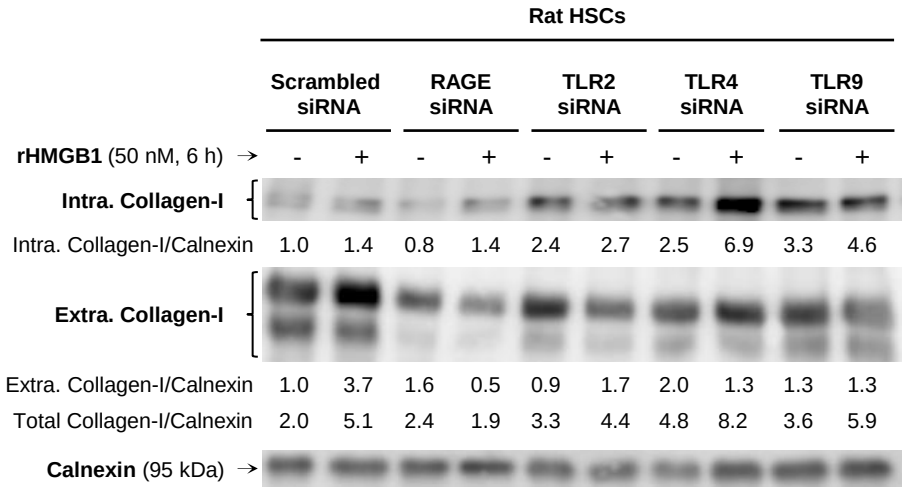

Supplementary Figure 2

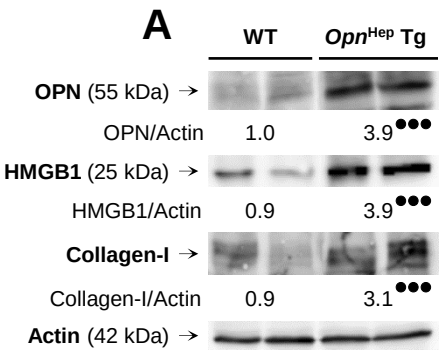

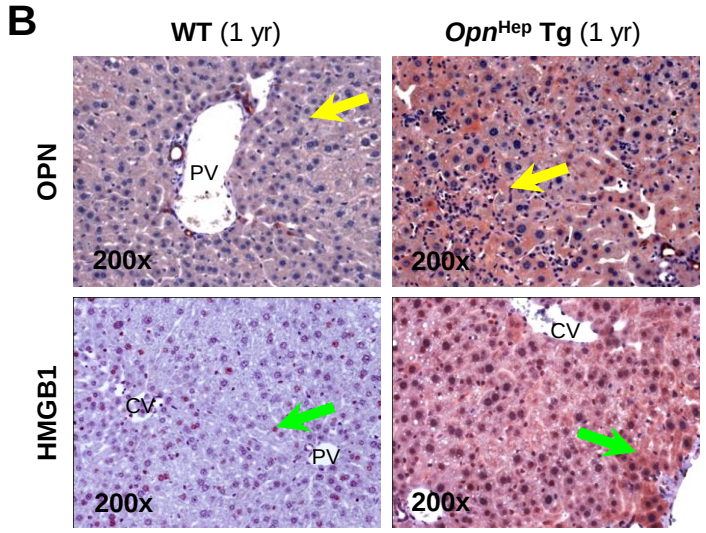

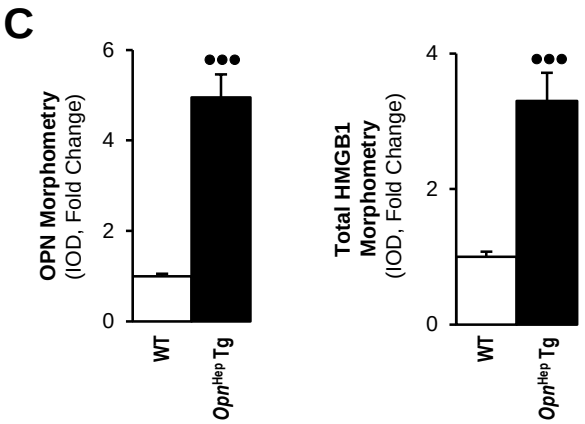

D

HMGB1	Nuclear	Cytoplasmic	Nuclear/Total	Cytoplasmic/Total
WT (1 yr)	1.0±0.1	1.0±0.0	0.7±0.0	0.2±0.0
***Opn*^{Hep} Tg** (1 yr)	1.8±0.3••	4.8±0.8•••	0.6±0.0••	0.4±0.0••

Supplementary Figure 3

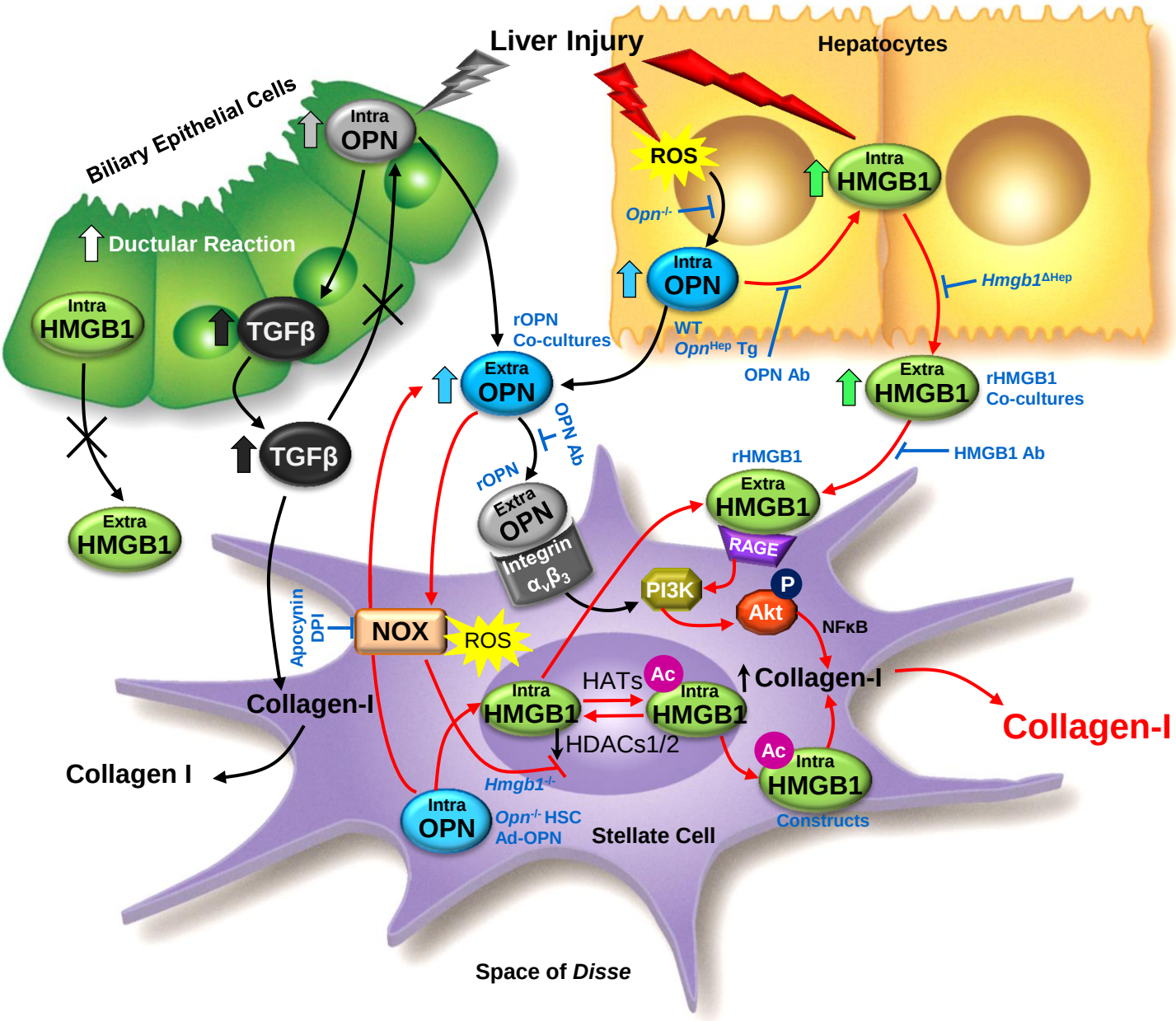

Supplementary Figure 4